the compact phase, appears in *J. Phys. (Paris)* **51**, 2653 (1990).
13. T. Hwa, thesis, Massachusetts Institute of Technology (1990).
14. S. Leibler and A. C. Maggs, *Phys. Rev. Lett.* **63**, 406 (1989).
15. M. Kardar, *Nucl. Phys. B* **5A**, 209 (1988).
16. See, for example, (*1*) and references therein.
17. For example, see the review by S. Dietrich on wetting phenomena in *Phase Transitions and Critical Phenomena*, C. Domb and J. L. Lebowitz, Eds. (Academic Press, London, 1988), vol. 12, chap. 1.
18. F. F. Abraham, *Homogeneous Nucleation Theory* (Academic Press, New York, 1974), sect. 3.7 and chap. 6; _____ and J. Canosa, *J. Chem. Phys.* **50**, 1303 (1969).
19. J. Toner, *Phys. Rev. Lett.* **64**, 1741 (1990).
20. F. F. Abraham, in preparation.
21. We have benefited from conversations with D. R. Nelson. F.F.A. acknowledges a probing comment by J. S. Langer that led to the simulation of the "zipper" transition in the model membrane with attraction being restricted to the rim particles of the membrane. Research by M.K. was supported by NSF grant DMR-90-01519.

10 October 1990; accepted 14 January 1991

The Shapes and Sizes of Closed, Pressurized Random Walks

JOSEPH RUDNICK AND GEORGE GASPARI

Two-dimensional cell-like membranes acted on by osmotic pressure differentials are represented by closed, unrestricted random walks. The treatment omits excluded-volume effects, and the pressure that is imposed thus favors an oriented area, so that the shriveled configuration of a vesicle with excess external pressure is inaccessible in this model. Nevertheless, the approach has the decided advantage of yielding analytic expressions in a complete statistical analysis. Results are presented for the average square of the radius of gyration, the asphericity, and the probability distribution of the principal components of the radius of gyration tensor. The analysis is done in both the constant-pressure and constant-area ensembles.

TWO-DIMENSIONAL VESICLES, AS modeled by Leibler and colleagues (*1*), consist of closed, self-avoiding chains that encircle a two-dimensional volume. If one introduces a pressure differential between the enclosed volume and the region surrounding the vesicle, one has a model for cell-like structures subject to osmotic forces. Numerical studies reveal the existence of three different regimes of vesicle conformations and a catastrophic transition as the difference between the internal and the external pressure is varied (*2, 3*). When this difference is sufficiently large and negative, the vesicles become severely deflated. The walls of the shriveled vesicles resemble tree-like structures. In fact, the walls appear to be governed by the statistics of branched, excluded-volume polymers. When the pressure differential is close to zero, the vesicles are flaccid. The scaling laws governing the wall conformations are those of simple, closed, self-avoiding walks. As the pressure differential is increased to a sizable positive value, the vesicles inflate and increasingly resemble two-dimensional inflated balloons. At a critical value of the pressure differential, the vesicles share the fate of the overinflated balloon and explode, unless the walls are made of extremely rigid segments. These studies (*1–3*) also have investigated the shape distributions and scaling properties of vesicles and their walls in these three regimes.

We now report the results of calculations of a number of properties of two-dimensional vesicles with non–self-avoiding walls. We have discovered that removing the excluded-area restriction transforms the pressurized vesicle system from a model whose specific properties can only be obtained numerically to one that is completely solvable. We have obtained explicit expressions for various important properties, including the full combined distribution function for the principal radii of gyration of vesicles under the influence of excess internal pressure. We also have obtained results for vesicle sizes and shapes in the conjugate constant-area ensemble.

We investigated the scaling properties of the two-dimensional vesicle with non–self-avoiding walls and found that the scaling forms proposed by Leibler *et al.* (*1*) hold in the corresponding regimes of our simpler model. Although allowing vesicle walls to intersect ignores a fundamental physical restriction on the allowed conformations of real membranes, we hold that the extreme tractability of this model more than offsets the disadvantages resulting from the tenuousness of its connection to real, three-dimensional vesicles. In addition, we anticipate that the results reported here will be the zeroth-order results on which one can hope to improve with the use of the powerful new techniques that have been applied to various two-dimensional systems.

J. Rudnick, Department of Physics, University of California, Los Angeles, CA 90024.
G. Gaspari, Department of Physics, University of California, Santa Cruz, CA 95064.

The vesicles we studied have walls consisting of N linear links, or displacements, $\boldsymbol{\eta}_i$ ($1 \leq i \leq N$). The walls are closed, so that $\Sigma\boldsymbol{\eta}_i = 0$. The links are, in the absence of a pressure differential, governed by a simple Gaussian distribution in that the probability that the link $\boldsymbol{\eta}_i$ has a length between η and $\eta + d\eta$ is proportional to $\exp(-\eta^2)d\eta$. The influence of the pressure differential p is felt through the following additional contribution to the probability distribution:

$$P_A(\boldsymbol{\eta}_i) = e^{-pA} \quad (1)$$

where A is the oriented area of the closed wall; this is to say that A is given by the integral $\frac{1}{2}\oint(y\,dx - x\,dy)$ taken along the wall in the direction of increasing index i. Notice that if the vesicle is flipped over the area defined in this way changes sign. A vesicle with a higher pressure inside than outside will tend to inflate (in a particular sense). A vesicle with a negative pressure differential will inflate in the opposite sense. There is no deflated phase. Furthermore, "figure eight" and more complicated configurations in which the vesicle walls cross will occur. Thus in this model a pressure differential has the effect of discouraging "wrong" sense configurations.

The distribution function governing individual link lengths is also taken to be Gaussian. In this respect, the statistics of the bounding surface are those of a closed,

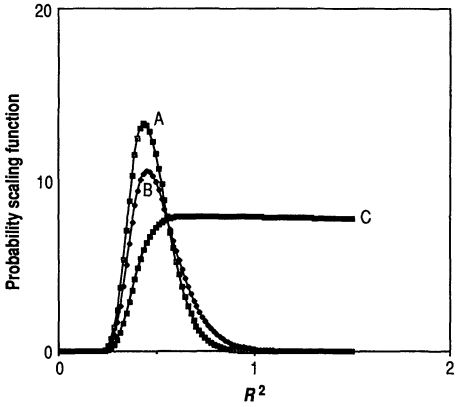

Fig. 1. Probability distribution scaling function, $\mathcal{P}(R^2N^{-2\nu}, x^{2\nu})$ (see Eq. 11), plotted against R^2 for (curve A) $p \ll p_c$, (curve B) $p = p_c/2$, and (curve C) $p = 0.999p_c$. The vertical scale is enhanced by a factor of 200 in the case of curve C.

random-flight chain. The key to the solution of the vesicle problem is the recognition that the pressure differential as specified by Eq. 1 leaves the Gaussian form unaltered. This result follows because of the bilinear form of the overall distribution

$$P(\boldsymbol{\eta}_i) = \exp\left(-\sum_{i=1}^{N}\frac{\eta_{ix}^2+\eta_{iy}^2}{\Delta^2}\right)$$
$$\exp\left[-\frac{p}{2}\sum_{ij}\eta_{iy}\eta_{jx}\varphi(i-j)\right] \quad (2)$$

where $\varphi(i)$ is a step function [$\varphi(i) = 1$ when $i \geq 0$ and -1 when $i < 0$] and Δ is the average length of a link in the absence of pressure. This Gaussian form is easily diagonalized on choosing a new basis set for the $\boldsymbol{\eta}_i$ variables. We write

$$\eta_{ix} = \sum_k A_k\sqrt{\frac{2}{N}}\cos ki + \sum_k B_k\sqrt{\frac{2}{N}}\sin ki + \frac{1}{\sqrt{N}}A_0 \quad (3)$$

and

$$\eta_{iy} = \sum_k A_k'\sqrt{\frac{2}{N}}\cos ki + \sum_k B_k'\sqrt{\frac{2}{N}}\sin ki + \frac{1}{\sqrt{N}}A_0 \quad (4)$$

where $k = 2\pi\ell/N$, ℓ being an integer. Because the wall around the vesicle is closed, both components of the displacements are constrained to add up to zero, and thus $A_0 = A_0' = 0$. In terms of the amplitudes on the right side of Eqs. 3 and 4, the probability distribution is given by

$$P(A, A', B, B') = \exp\left(-\sum_k\frac{A_k^2+A_k'^2+B_k^2+B_k'^2}{\Delta^2} - p\sum_k\frac{B_kA_k' - A_kB_k'}{k}\right) \quad (5)$$

The shapes assumed by the vesicle will be described in terms of the eigenvalues of the 2×2 gyration tensor $\mathbf{T}$ (*4, 5*). The radius of gyration tensor, which quantifies the distances that an object extends in various directions about its center of mass, is perhaps most familiar in the context of rigid body rotation. It is central to the calculation of the moments of inertia of a nonspherical object. In terms of A_R and B_R variables it can be shown that, in the limit of large N (*6*),

$$T_{xx} = \sum_k\frac{1}{Nk^2}(A_k^2+B_k^2) \quad (6)$$

$$T_{yy} = \sum_k\frac{1}{Nk^2}(A_k'^2+B_k'^2) \quad (7)$$

$$T_{xy} = T_{yx} = \sum_k\frac{1}{Nk^2}(A_kA_k'+B_kB_k') \quad (8)$$

We can now proceed to calculate various key quantities. In the remainder of this discussion we quote some of the results that have been obtained up to now. A more complete discussion of this work will be presented (*6*). From the above equations, we have been able to obtain analytic expressions for the average radius of gyration and the asphericity parameter of vesicles, the distribution function of its mean radius of gyration, and a closed-form expression for the full distribution of the principal radii of gyration of the vesicle with excess internal pressure.

Because the last result contains all the other information listed above, it is presented first. In two dimensions, an exact formula for the distribution of the principal radii of gyration is

$$\int\delta(\lambda_1+\lambda_2-T_{xx}-T_{yy})\,\delta\,[(\lambda_1-\lambda_2)^2 - (T_{xx}-T_{yy})^2 - 4T_{xy}^2]$$
$$P(A, A', B, B')\,d[A]\ldots d[B'] \quad (9)$$

where the integral is over all the Fourier components. By using Fourier representations of the Dirac δ functions, the integration can be carried out, reducing $P(\lambda_1, \lambda_2; p)$ to quadrature (*7*). An explicit expression for $P(R^2)$, the full distribution of the mean radius of gyration $\lambda_1 + \lambda_2 = R^2$, is easily obtained from the above result, yielding

$$P(R^2) = \frac{4\pi^2}{N}\frac{1}{x}\sum_{n=-\infty}^{\infty}(2n-x)\,n\,(n-x)\exp\left[-\frac{4\pi R^2}{N}n\,(n-x)\right] \quad (10)$$

where N is the number of wall segments of the vesicle and x is the ratio p/p_c, p_c being the critical pressure differential at which the vesicle bursts. This pressure has the value $4\pi/N\Delta^2$. In light of the way in which N enters into Eq. 10, it is a straightforward matter to verify that $P(R^2)$ has the scaling form

$$P(R^2) = N^{-2\nu}\,\mathcal{P}(R^2N^{-2\nu}, x^{2\nu}) \quad (11)$$

This is entirely consistent with the proposals of Leibler and colleagues (*1*). Figure 1 is a plot of $\mathcal{P}(R^2N^{-2\nu}, x^{2\nu})$ for three different values of x. The vertical scale has been greatly enhanced for the case $x = 0.999$.

Simple closed-form results for the size and, indirectly, the shape of the vesicles under consideration can now be obtained. For $\langle R^2\rangle$, the expectation value of the mean square radius of gyration, we have, in the constant pressure ensemble,

$$\langle R^2\rangle = \frac{\Delta^2N}{4\pi^2}\left[\frac{1}{x^2} - \frac{\pi}{x\tan(\pi x)}\right] \quad (12)$$

where, again, $x = p/p_c$. It is also possible to obtain a result for $\langle R^2\rangle$ in the constant-area ensemble. To do this, we use the Fourier transform of the Dirac δ function and take advantage of the fact that the pressure can be given an imaginary value in Eqs. 1, 2, and 5. The end result of the calculations is the following expression for $\langle R^2\rangle$:

$$\langle R^2\rangle = \frac{N\Delta^2}{2\pi}\cosh^2\left(\frac{2\pi A}{N\Delta^2}\right)\left[\frac{2}{\pi}\ln\left(1+e^{-4\pi A/N\Delta^2}\right) + \frac{8A}{N\Delta^2}\frac{e^{-4\pi A/N\Delta^2}}{1+e^{-4\pi A/N\Delta^2}}\right] \quad (13)$$

It is a straightforward matter to verify that, as the area in Eq. 13 goes to infinity, $\langle R^2\rangle$ approaches A/π. Infinite area vesicles are dominantly circular. This limit for the shape of the infinite vesicle also should be approached in the constant-pressure ensemble as $x \to 1^-$ or $p \to p_c^-$. A separate calculation in that ensemble yields the exact relation

$$\langle A\rangle = pN\Delta^2\langle R^2\rangle/4 = \pi p\langle R^2\rangle/p_c \quad (14)$$

so that the expected limiting shape is indeed approached when the vesicle is on the verge of exploding. It is important to emphasize that the constant-area ensemble is not equivalent to the constant-pressure ensemble in the thermodynamic sense. This is evident if one compares the plots of $\langle R^2\rangle$ against A in the constant-area ensemble with the plot of $\langle R^2\rangle$ against $\langle A\rangle$ in the constant-pressure ensemble (Fig. 2). Although both plots are asymptotically linear with a slope of $1/\pi$, as the area and mean radius of

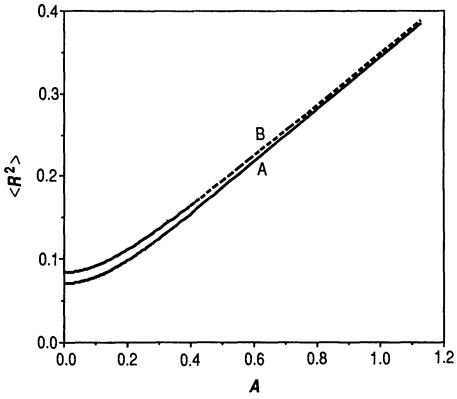

Fig. 2. $\langle R^2\rangle$ plotted against A (or $\langle A\rangle$) for (curve A) constant-area ensemble and (curve B) constant-pressure ensemble. The slopes of both curves approach $1/\pi$ asymptotically.

gyration approach infinity, they are by no means identical at moderate values of those quantities. Both plots exhibit scaling behavior in that both $\langle R^2 \rangle$ and A (or $\langle A \rangle$) scale with $N^{2\nu}$.

Finally, we turn to the asphericity parameter A_2 (*8, 9*), which provides a direct measure of the deviation from a sphere of the vesicles' shapes. In terms of the eigenvalues of $\mathbf{T}$, $A_2 = (\lambda_1 - \lambda_2)^2/(\lambda_1 + \lambda_2)^2$. In the constant-pressure ensemble, after a rather tedious calculation, we find

$$A_2 = \left[\frac{8}{p^4} - \frac{N^2}{6p^2} - \frac{2N}{p^3 \tan\left(\frac{Np}{4}\right)}\right] \Bigg/ \left[-\frac{8}{p^4} - \frac{N^2}{6p^2} + \frac{N^2}{2p^2 \sin^2\left(\frac{Np}{4}\right)}\right] \quad (15)$$

In the limit $p = 0$, the asphericity approaches 1/3. This limiting value is consistent with earlier results for the average shape of a closed, non–self-avoiding random walk. As the pressure approaches its critical value ($p \rightarrow p_c$), the right side of Eq. 15 approaches zero, as expected. A similar calculation can be done for the constant-area ensemble.

Although the results presented here are new and interesting in their own right, they become particularly pertinent when used as the starting point for an excluded-volume calculation, a problem that has proven to be analytically intractable. The approach outlined here is useful for studying the dynamic behavior of vesicles under pressure (*6*).

REFERENCES AND NOTES

1. S. Leibler, R. P. R. Singh, M. E. Fisher, *Phys. Rev. Lett.* **59**, 1989 (1987).
2. J. Camacho and M. E. Fisher, *ibid.* **65**, 9 (1990).
3. A. C. Maggs, S. Leibler, M. E. Fisher, J. Camacho, *Phys. Rev. A*, in press.
4. K. Solc and W. H. Stockmayer, *J. Chem. Phys.* **54**, 2756 (1971).
5. G. Gaspari, J. Rudnick, A. Beldjenna, *J. Phys. A* **20**, 3393 (1987).
6. G. Gaspari, A. Beldjenna, J. Rudnick, in preparation.
7. For the case $p = 0$, we have simply the case of unrestricted random walks, where the exact results of K. Solc and W. Gobush [*Macromolecules* 7, 814 (1974)] pertain. These investigators arrive at an exact expression for $P(\lambda_1 \lambda_2; 0)$ by a somewhat indirect procedure, yielding an expression for which numerical results cannot be readily obtained.
8. J. Rudnick and G. Gaspari, *J. Phys. A* **19**, L191 (1986).
9. J. Aronovitz and D. R. Nelson, *J. Phys. (Paris)* **47**, 1445 (1986).

30 October 1990; accepted 14 January 1991

A Virus-Encoded "Superantigen" in a Retrovirus-Induced Immunodeficiency Syndrome of Mice

AMBROS W. HÜGIN, MELANIE S. VACCHIO, HERBERT C. MORSE III*

The development of an immunodeficiency syndrome of mice caused by a replication-defective murine leukemia virus (MuLV) is paradoxically associated with a rapid activation and proliferation of CD4$^+$ T cells that are dependent on the presence of B cells. The responses of normal spleen cells to B cell lines that express the defective virus indicated that these lines express a cell surface determinant that shares "superantigenic" properties with some microbial antigens and Mls-like self antigens. This antigen elicited a potent proliferative response that was dependent on the presence of CD4$^+$ T cells and was associated with selective expansion of cells bearing $V_\beta 5$. This response was markedly inhibited by a monoclonal antibody specific for the MuLV *gag*-encoded p30 antigen.

INFECTION OF CERTAIN STRAINS OF mice with a mixture of replication-competent and replication-defective MuLV induces the disorder murine acquired immunodeficiency syndrome (MAIDS) (*1–6*), which is characterized by polyclonal activation and proliferation of T and B cells (*1*), severe immunodeficiency (*1*), aberrant regulation of cytokines (*1, 3*), enhanced susceptibility to infection (*4*), and late B cell lineage lymphomas in some animals (*5*). The defective virus in this mixture is required for development of disease (*6*) and can induce the syndrome if administered without helper MuLV (*7*).

Previous studies showed that complex interactions between T and B cells were required for induction of the full spectrum of immunologic abnormalities that characterize mice with MAIDS. T cells of the CD4$^+$ subset are required for induction of B cell activation, differentiation to immunoglobulin (Ig) secretion, and impaired responses to mitogenic and antigenic stimuli as well as for functional abnormalities of CD8$^+$ T cells (*8*). Conversely, mature B cells are required in vivo for induction of CD4$^+$ and CD8$^+$ T cell dysfunction (*9*).

We suggested previously that this interlocking activation of different components of the immune system may be due to stimulation of T cells by determinants expressed on the surface of B cells that have features of "superantigens" with the Pr60^{gag} of the defective virus as one candidate (*9*). Superantigens of microbial origin (*10–12*) (such as staphylococcal toxins and *Mycoplasma arthriditis* mitogen) or self origin (*10, 13–15*) (Mls-like products) have the ability to stimulate large numbers of T cells by virtue of their capacity to engage T cell receptors (TCRs) bearing particular variable region sequences of the TCR β chain (V_β), almost regardless of the contributions of other portions of the β or α chain to the structure of the TCR (*10–16*). The activity of these antigens is also dependent on the simultaneous expression of class II proteins on antigen presenting cells (APC) (*10–16*).

To evaluate this model, we took advantage of cultured cell lines derived from B cell lineage lymphomas that developed late in the course of MAIDS. Two lines, B6-1153 and B6-1710, were recovered from tumors of B6 mice and B6xCBA/N-2252 from an infected (B6 × CBA/N)F_1 mouse (*5*). All three lines have acquired multiple copies of the defective virus, but differ in the extent to which these genomes are expressed (*17*). For the lines studied most intensively, B6-1710 expressed *gag* polyproteins encoded by defective and nondefective viruses at concentrations readily detectable with monoclonal antibodies to p12 (anti-p12) and p30 (anti-p30) in flow cytometry analyses (Fig. 1A, inset), whereas B6-1153 expressed very little, if any (Fig. 1B, inset); B6xCBA/N-2252 was quite similar to B6-1710 for expression of *gag*-encoded antigens (*18*). All three lines expressed major histocompatibility complex (MHC) class II proteins comparably and at amounts higher than on most normal B cells (*18*).

After irradiation and cocultivation with normal B6 spleen cells, B6-1710 stimulated a vigorous proliferative response in a cell dose-dependent fashion (Fig. 1A) and at concentrations equivalent to those obtained with mitogenic lectins. Similar results were obtained when irradiated B6xCBA/N-2252 cells were used to stimulate normal F_1 spleen cells (*18*). In contrast, the low p12- and p30-expressing line, B6-1153, induced

A. W. Hügin and H. C. Morse III, Laboratory of Immunopathology, National Institute of Allergy and Infectious Diseases, NIH, Bethesda, MD 20892.
M. S. Vacchio, Experimental Immunology Branch, National Cancer Institute, NIH, Bethesda, MD 20892.

*To whom correspondence should be addressed at Building 7, Room 304, NIH, Bethesda, MD 20892.